

PNAS

www.pnas.org

Supplementary Information for

Staphylococcal protein A inhibits complement activation by interfering with IgG hexamer formation

Ana Rita Cruz^{1,†}, Maurits A. den Boer^{2,†}, Jürgen Strasser³, Seline A. Zwarthoff¹, Frank J. Beurskens⁴, Carla J. C. de Haas¹, Piet C. Aerts¹, Guanbo Wang^{2,5}, Rob N. de Jong⁴, Fabio Bagnoli⁶, Jos A. G. van Strijp¹, Kok P. M. van Kessel¹, Janine Schuurman⁴, Johannes Preiner³, Albert J. R. Heck^{2,#} & Suzan H. M. Rooijackers^{1,#,*}

¹Medical Microbiology, University Medical Center Utrecht, Utrecht University, Utrecht, The Netherlands

²Bijvoet Center for Biomolecular Research and Utrecht Institute for Pharmaceutical Sciences, Utrecht University, Padualaan 8, 3584 CH Utrecht, The Netherlands

³University of Applied Sciences Upper Austria, 4020 Linz, Austria

⁴Genmab, Utrecht, The Netherlands

⁵School of Chemistry and Materials Science, Nanjing Normal University, Nanjing 210023, China

⁶GSK Siena, Italy

[†]These authors contributed equally to this work as first authors

[#]These authors shared supervision of this study

^{*}Corresponding author.

Email: s.h.m.rooijackers@umcutrecht.nl

This PDF file includes:

Supplementary text Materials and methods
Figures S1 to S8
Tables S1 to S5
SI References

Supplementary text Materials and Methods

Production and purification of human monoclonal antibodies

Monoclonal antibodies against DNP (DNP-G2a2) used for MS, HS-AFM and QCM experiments were recombinantly expressed as wild-type and hexamer-forming RGY mutant (1) IgG1, IgG2, IgG3 and IgG4 and obtained from Genmab (Utrecht, the Netherlands) (2, 3).

For the other experiments of this study, we used human monoclonal antibodies produced recombinantly in human Expi293F cells (Life Technologies) as described before (4), with minor modifications. Briefly, gBlocks (Integrated DNA technologies, IDT), containing codon-optimized variable heavy and light chain (VH and VL) sequences with an upstream KOZAK and HAVT20 signal peptide, were cloned into homemade pcDNA34 vectors, upstream the IgG heavy and kappa light chain constant regions, respectively, using Gibson assembly (New England Biolabs). The VH and VL sequences of the antibodies were derived from previously reported antibodies anti-DNP (DNP-G2a2) (5) and anti-WTA GlcNAc- β -4497 (patent WO/2014/193722) (6) (Table S5). Transfection of EXPI293F cells was performed using PEI (Polyethylenimine HCl MAX; Polysciences). After 4 to 6 days of transfection, IgG1, IgG2 and IgG4 antibodies were isolated from cell supernatants using a HiTrap Protein A High Performance column (GE Healthcare), whereas IgG3 antibodies were isolated with a HiTrap Protein G High Performance column (GE Healthcare). Antibodies were dialyzed in PBS, overnight at 4 °C, and filter-sterilized through 0.22 μ m Spin-X filters. Antibodies were analyzed by size exclusion chromatography (GE Healthcare) and monomeric fractions were isolated in case of aggregation levels >5%. The concentration of the antibodies was determined by measurement of the absorbance at 280 nm and antibodies were stored at -20 °C until use. The anti-HIa (MEDI4893; patent WO/2017/075188A2), which served as a control, was a gift from Dr Alexey Ruzin, MedImmune (AstraZeneca).

Cloning, expression and purification of SpA-B constructs

Codon-optimized gBlocks (IDT) for wild-type B domain of SpA (SpA-B), SpA-B lacking Fc-binding properties (SpA-B^{KK}; Q9K and Q10K mutations) and SpA-B lacking Fab-binding properties (SpA-B^{AA}; D36A and D37A mutations) (Table S1), containing a C-terminal LPETG sortagging sequence, were cloned into a modified pRSET-C-HIS vector by Gibson assembly. Recombinant proteins, containing a C-terminal LPETGG-AAA-HHHHHH tag, were generated in *E. coli* BL21(DE3) and were isolated under native purification conditions using a 5 HisTrap High Performance Column (GE Healthcare) with imidazole gradient (10-250 mM; Sigma-Aldrich). SpA-B constructs were dialyzed in 50 mM Tris 300 mM NaCl pH 8.0, overnight at 4 °C, and stored at -20 °C until use.

Antibody cleavage

Anti-CD52, anti-WTA and anti-HIa IgG1 Fc and F(ab')₂ molecules were generated by overnight digestion at 37 °C using 0.25 U/μg FabRICATOR IdeS (Genovis AB).

FITC-conjugated rabbit F(ab')₂ anti-human C1q was obtained by digestion of FITC-conjugated rabbit anti-human C1q (Dako) using 1 U/μg of recombinant His-tagged IdeS protease. After incubation of antibody with IdeS for 2 h at 37 °C in the dark, F(ab')₂ fragment was purified through HiTrap Protein A High Performance column (GE Healthcare) and HiTrap High Performance column (GE Healthcare).

Antibody labeling

IgG labeling was performed by incubation of antibodies with Alexa Fluor⁶⁴⁷ NHS Ester (Succinimidyl Ester; ThermoFisher Scientific). In detail, 1 μL of 10 mg/mL Alexa Fluor⁶⁴⁷ NHS Ester was added to 100 μL of 1 mg/mL antibody in PBS with 0.1 M sodium bicarbonate buffer. After 2 h incubation at RT in the dark, labeled antibodies were separated from the free probe by use of Pierce desalting spin column 0.5 mL (ThermoFisher Scientific), according to the manufacturer's manual. Subsequently, absorbance was measured at 280 nm for protein and 647 nm for the probe, using a Nanodrop.

Binding of antibodies to beads coated with SpA constructs

Dynabeads His-Tag Isolation & Pulldown (Invitrogen) were washed in PBS-TH (PBS, 0.05% (v/v) Tween-20 and 0.5% human serum albumin (HSA)). 50 μL of 30 μg/mL his-tagged SpA-B, SpA-B^{KK} or SpA-B^{AA} was mixed with 1 μL beads for 30 min at 4 °C, shaking (± 700 rpm). After two washes with PBS-TH, 0.05 μL beads were incubated with 2 μg/mL anti-DNP IgG1, anti-DNP IgG3 or anti-WTA IgG1 in 30 μL, for 30 min at 4 °C, shaking (± 700 rpm). A VH3-type antibody, anti-HIa IgG1, was included as a control for Fab binding to both SpA-B and SpA-B^{KK}. Anti-DNP IgG3 was included as a negative control. All antibodies were also incubated with Dynabeads Protein G (Invitrogen) that served as reference binding for all antibodies, including IgG3. Antibody binding was detected using directly labeled IgG or Alexa Fluor⁶⁴⁷-conjugated goat F(ab')₂ anti-human kappa (Southern Biotech). Samples were measured using flow cytometry (BD FACSVerser) and data, based on a single bead population, were analyzed using FlowJo software. Mean fluorescence values were expressed relative to the control binding to Protein G beads for each antibody.

Enzyme-Linked Immunosorbent Assay (ELISA)

MaxiSorp plates (Nunc) were coated with 3 μg/mL SpA-B or SpA in 0.1 M sodium carbonate, overnight at 4 °C. The day after, plates were washed three times with PBS-T (PBS, 0.05% (v/v) Tween-20) and blocked with 4% bovine serum albumin (BSA) in PBS-T, for 1 h at 37 °C. The following incubations were performed for 1 h at 37 °C followed by 3 washes with PBS-T. Five-fold

serial dilutions (starting from 20 nM) of human monoclonal anti-DNP IgG1, IgG2, IgG3 and IgG4 in 1% BSA in PBS-T were added to the wells. Bound antibodies were detected with horseradish peroxidase (HRP)-conjugated goat F(ab')₂ anti-human kappa (Southern Biotech) in 1% BSA in PBS-T and Tetramethylbenzidine (TMB) as substrate. The reaction was stopped with 1N sulfuric acid and absorbance was measured at 450 nm in the iMark™ Microplate Absorbance Reader (Bio-Rad).

DNP labeled liposomes

DNP-labeled liposomes consisting of 1,2-dipalmitoyl-sn-glycero-3-phosphocholine (DPPC), 1,2-dipalmitoyl-sn-glycero-3-phosphoethanolamine (DPPE) and 1,2-dipalmitoyl-sn-glycero-3-phosphoethanolamine-N-[6-[(2,4-dinitrophenyl)amino]hexanoyl] (DNP-cap-DPPE) were used to generate supported lipid bilayers (SLBs) on mica and SiO₂ substrates. The lipids were purchased from Avanti Polar Lipids, mixed at a ratio of DPPC:DPPE:DNP-cap-DPPE = 90:5:5 (molar ratio), and dissolved in a 2:1 mixture of chloroform and methanol. After the solvents were rotary-evaporated for 30 min, the lipids were again dissolved in chloroform, which was then rotary-evaporated for 30 min. Drying was completed at a high vacuum pump for 2 h. The lipids were dissolved in 500 μL Milli-Q H₂O while immersed in a water bath at 60 °C, flooded with argon, and sonicated for 3 min at 60 °C to create small unilamellar vesicles. These were diluted to 2 mg/mL in buffer #1 (10 mM HEPES, 150 mM NaCl, 2 mM CaCl₂, pH 7.4) and frozen for storage using liquid N₂.

IgG oligomer statistics on DNP-SLBs

For experiments studying the effect of SpA constructs, the incubation step with SpA proceeded for at least 2 h at 37 °C. IgG-RGY was used at a total IgG concentration of 2 μM in the presence or absence of 20 μM SpA-B or SpA. IgG oligomer distributions were then obtained by incubating DNP-SLBs with 33.3 nM of the respective IgG variant for 5 min, and analyzed in a two-step process: Individual particle dimensions were determined by HS-AFM, and the respective oligomeric states were further confirmed by observing their decay pattern determined in subsequent forced dissociation experiments as described (7). In brief, molecules are scanned in a nondisrupting manner to gauge their number, height, and shape. Subsequently, the scanning force exerted by the HS-AFM cantilever tip is increased to dissociate oligomers into their constituent IgGs. Geometric parameters and oligomer decay patterns are combined to assign each IgG assembly its oligomeric state.

DNP-coated beads assays

Dynabeads M-270 Streptavidin beads (Invitrogen) were washed in PBS-TH and incubated, 100 times diluted, with 1 μg/mL of biotinylated 2,4-dinitrophenol (DNP-PEG2-GSGSGSGK(Biotin)-NH₂,

Pepscan Therapeutics B.V.) in PBS-TH for 30 min at 4 °C, shaking (\pm 700 rpm). For each condition, 0.5 μ L of beads were used ($\sim 3 \times 10^5$ beads/condition). After two washes with PBS-TH, DNP-coated beads were incubated with 20 nM anti-DNP IgG or 2-fold serial dilutions of anti-DNP IgG (starting from 20 nM IgG), for 30 min at 4 °C, shaking (\pm 700 rpm). The following incubations steps were performed under shaking conditions (\pm 700 rpm) for 30 min at 4 °C unless stated otherwise. Additionally, after each incubation, beads were washed twice with PBS-TH or VBS-TH (Veronal Buffered Saline pH 7.4, 0.5 mM CaCl₂, 0.25 mM MgCl₂, 0.05% (v/v) Tween-20, 0.5% HSA), dependent on buffer used in the following incubation step. For antibody binding detection, IgG-bound DNP-beads were next incubated with 1 μ g/mL Alexa Fluor⁶⁴⁷-conjugated goat F(ab')₂ anti-human kappa (Southern Biotech) in PBS-TH. For SpA binding detection, IgG-bound DNP-coated beads were first incubated with 200 nM of recombinant His-tagged SpA-B or SpA (ProSpec) in PBS-TH. Subsequently, beads were incubated with 1 μ g/mL chicken anti-HexaHistidine antibody (Nordic) in PBS-TH, followed by incubation with R-Phycoerythrin (PE)-conjugated donkey F(ab')₂ anti-chicken (Jackson ImmunoResearch) diluted 1/500 in PBS-TH. For C1q binding experiments, IgG-bound DNP-coated beads were incubated with 1.3 nM of purified C1 (Complement Technology) or C1q (Complement Technology) alone, in combination with, or followed by incubation of 200 nM or 4-fold dilutions (starting from 1 μ M) of recombinant SpA-B or SpA in VBS-TH, for 30 min at 37 °C. C1q was detected by use of 4 μ g/mL FITC-conjugated rabbit F(ab')₂ anti-human C1q. The binding of antibody, SpA and C1q to the beads were detected using flow cytometry (BD FACSVerse) and data were analyzed based on single bead population using FlowJo software.

Depletion of IgG and IgM from human serum

Human serum pooled from 20 healthy donors was depleted of IgG and IgM as previously reported (8). Briefly, IgG and IgM were captured by affinity chromatography using HiTrap Protein G High Performance column (GE Healthcare) and CaptureSelect IgM Affinity Matrix (ThermoFisher Scientific), respectively. After depletion, antibodies and complement levels were quantified by ELISA and complement activity was measured by classical pathway and alternative pathway hemolytic assays. As IgG and IgM depletion results in partial co-depletion of C1q, Δ IgG/IgM serum was reconstituted with purified C1q (Complement Technology) to physiological levels (70 μ g/mL).

Statistical analysis

Statistical analysis was performed with GraphPad Prism v.8.3 software, using unpaired two-tailed t-test or one-way ANOVA as indicated in the figure legends. At least three experimental replicates were performed to allow statistical analysis.

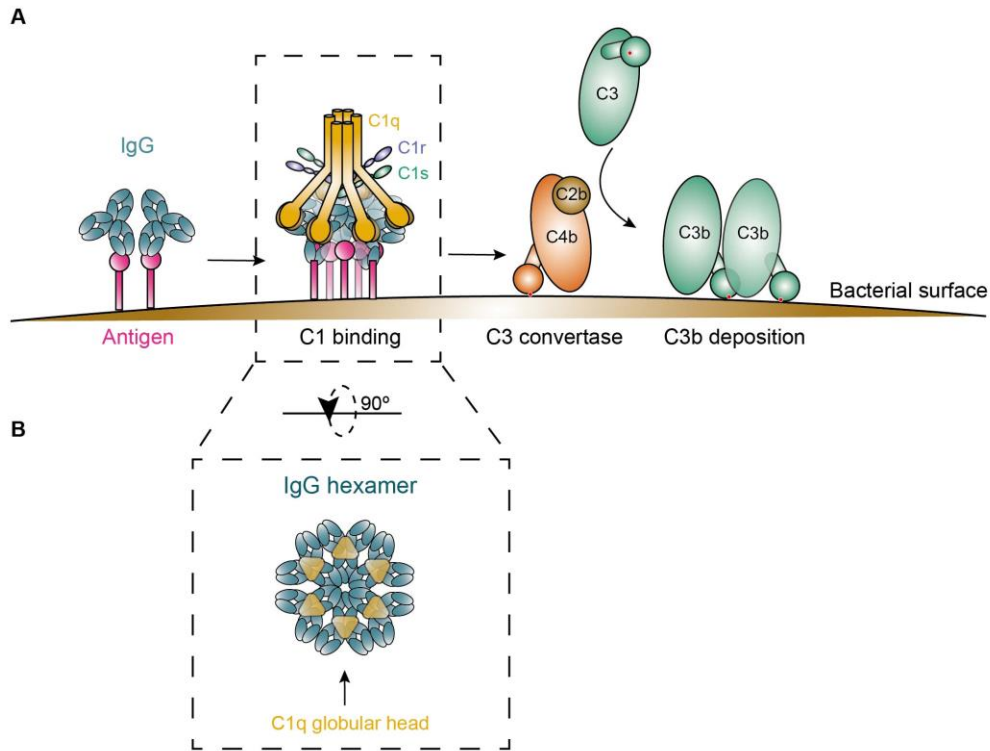


Fig. S1. Graphical representation of complement classical pathway activation. (A) Overview of complement classical pathway initiation. The fully assembled C1 complex binds to immune complexes on the bacterial surface, subsequently, its attached C1r/C1s proteases are activated and cleave C4 and C2 to generate C4b2b (C3 convertase). The C3 convertase cleaves C3 into C3b, which displays a previously hidden thioester that covalently binds to the bacterial surface. (B) The IgG hexameric rings, or IgG hexamers, are held together by non-covalent Fc-Fc interactions and form the docking platform for complement C1.

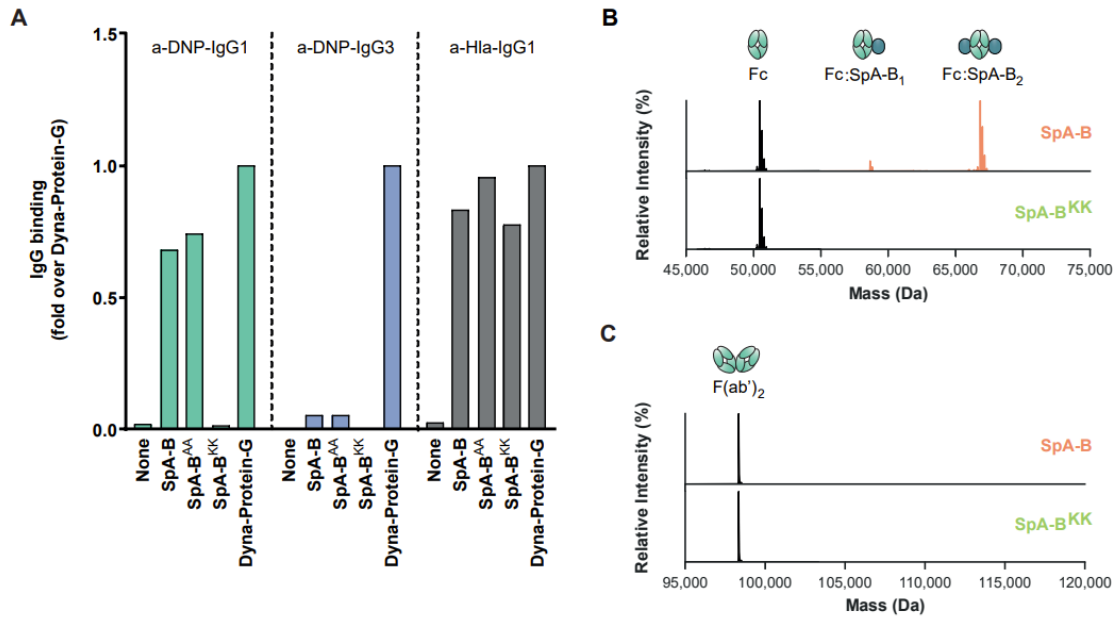


Fig. S2. Human anti-DNP antibodies only bind to SpA via their Fc region. (A) Binding of anti-DNP IgG1 (green), anti-DNP IgG3 (blue) and anti-Hla IgG1 (grey) to beads coated with His-tagged recombinant SpA-B (wild-type), SpA-B^{AA} (that only binds to IgG-Fc region), SpA-B^{KK} (that only binds to IgG-Fab region) or to Protein-G beads. Antibody binding was detected by the use of directly labeled IgG or Alexa Fluor⁶⁴⁷-conjugated goat F(ab')₂ anti-human kappa and was measured by flow cytometry. The anti-Hla IgG1 (VH3 family antibody) served as a control for Fab binding to SpA-B^{KK}. Protein G beads served as universal IgG1 and IgG3 binding control. (B, C) Deconvoluted native mass spectra of the Fc (B) and F(ab')₂ (C) molecules of anti-CD52 IgG1, resulting from IdeS digestion, in absence (black) or presence of SpA-B (orange) or SpA-B^{KK} (green). SpA-B binds to the Fc region, but not to Fab region. SpA-B^{KK} does not bind to the Fc or Fab region.

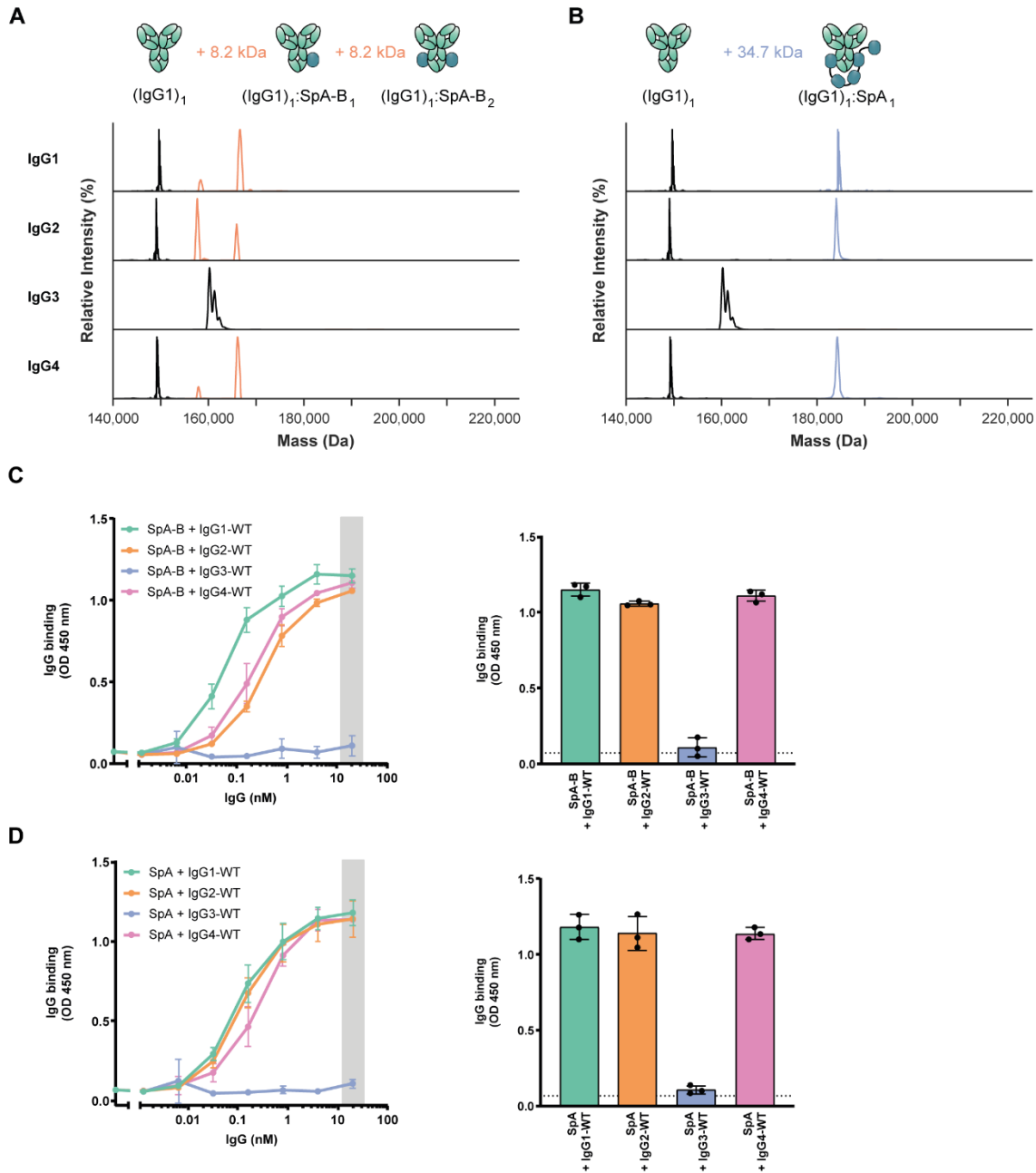


Fig. S3. Human IgG1, IgG2 and IgG4 bind to SpA, but not IgG3. (A, B) Deconvoluted native mass spectra revealing the binding stoichiometry of SpA-B (A) and SpA (B) with IgG. Incubation with SpA-B (orange) results in mass shifts corresponding to SpA-B binding to IgG1, IgG2 and IgG4 with up to 2:1 stoichiometry whereas SpA (blue) binds principally with 1:1 stoichiometry to the same IgG subclasses. Satellite peaks observed in the mass spectra of IgG3 result from the presence of additional O-glycosylation sites on the IgG3 hinge region. The top native MS spectra (human IgG1 binding to SpA-B or SpA) are the same as the spectra of Fig. 2. The cartoon regarding (IgG1)₁:SpA₁ binding is speculative, as it is still unknown which SpA domain interacts with which binding site on the IgG molecules. (C, D) Binding of the full concentration range of human IgG subclasses to SpA-

B (C) or SpA (D) coated on a 96-well plate. IgG binding was detected with HRP-labeled goat F(ab')₂ anti-human kappa. Bars represent the same data for the 20 nM IgG concentration only and the black dotted line shows the background absorbance from wells that were not incubated with IgG.

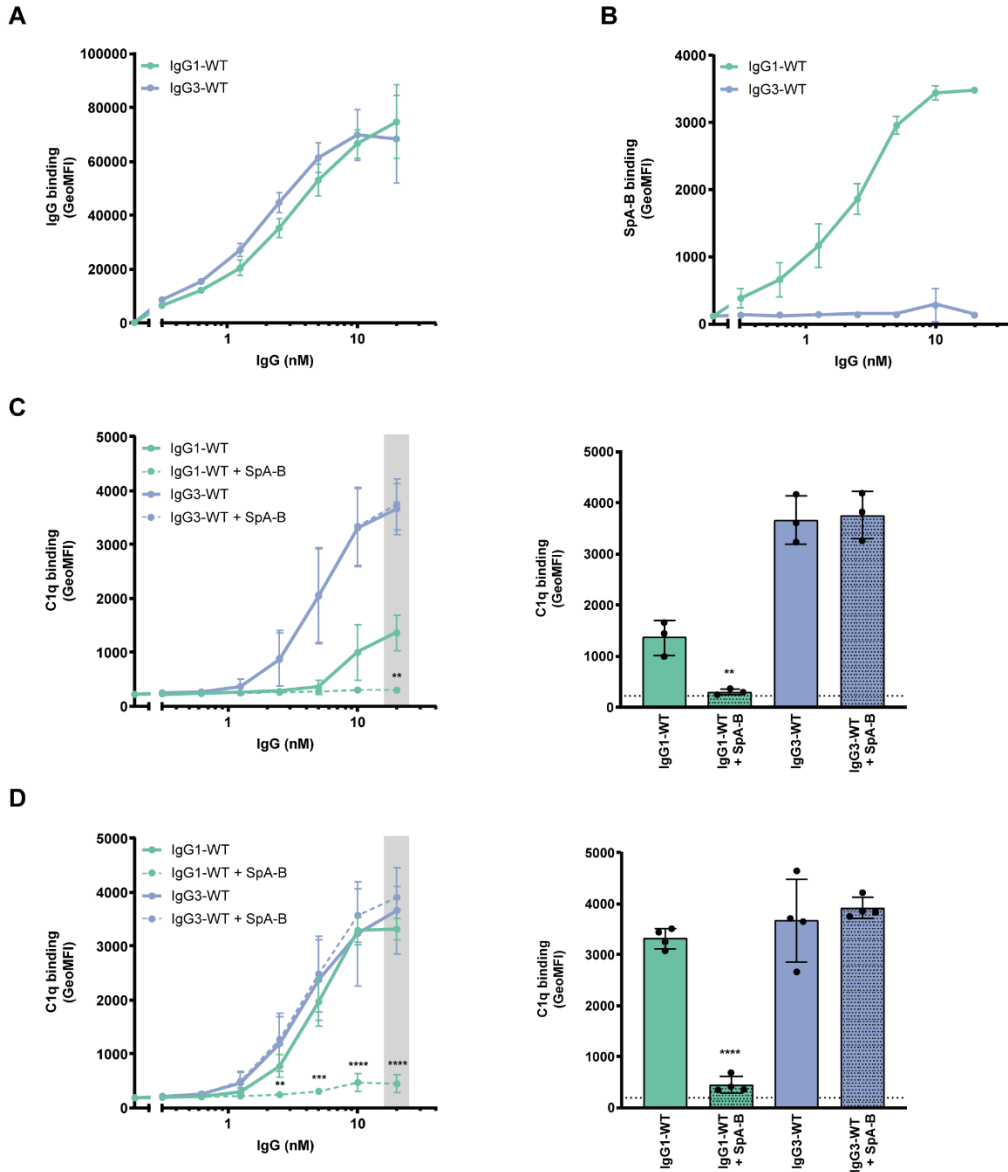


Fig. S4. The binding of SpA-B to antigen-bound IgG decreases C1q binding on target surfaces even if C1q is incubated before SpA-B. (A) Binding of anti-DNP IgG1-WT and IgG3-WT to DNP-coated beads, detected with Alexa Fluor⁶⁴⁷-conjugated goat F(ab')₂ anti-human kappa by flow-cytometry. (B) Binding of SpA-B to anti-DNP IgG1-WT and IgG3-WT bound to DNP-coated beads, detected with anti-HexaHistidine chicken antibody by flow cytometry. (C, D) C1q binding on IgG1-WT and IgG3-WT bound to DNP-coated beads, detected with FITC-conjugated rabbit F(ab')₂ anti-human C1q by flow-cytometry. Buffer (solid lines) or SpA-B (dotted lines) was added to the beads only after C1q (C) or C1 complex (D). Bars represent the same data for the 20 nM IgG concentration only and the black dotted line shows the background fluorescence from beads that were not incubated with IgG. Data are presented as geometric means \pm SD of three or four independent experiments. Statistical analysis was performed using an unpaired two-tailed t-test to compare

buffer and SpA-B conditions and showed when significant as **P < 0.01, ***P < 0.001 and ****P < 0.0001.

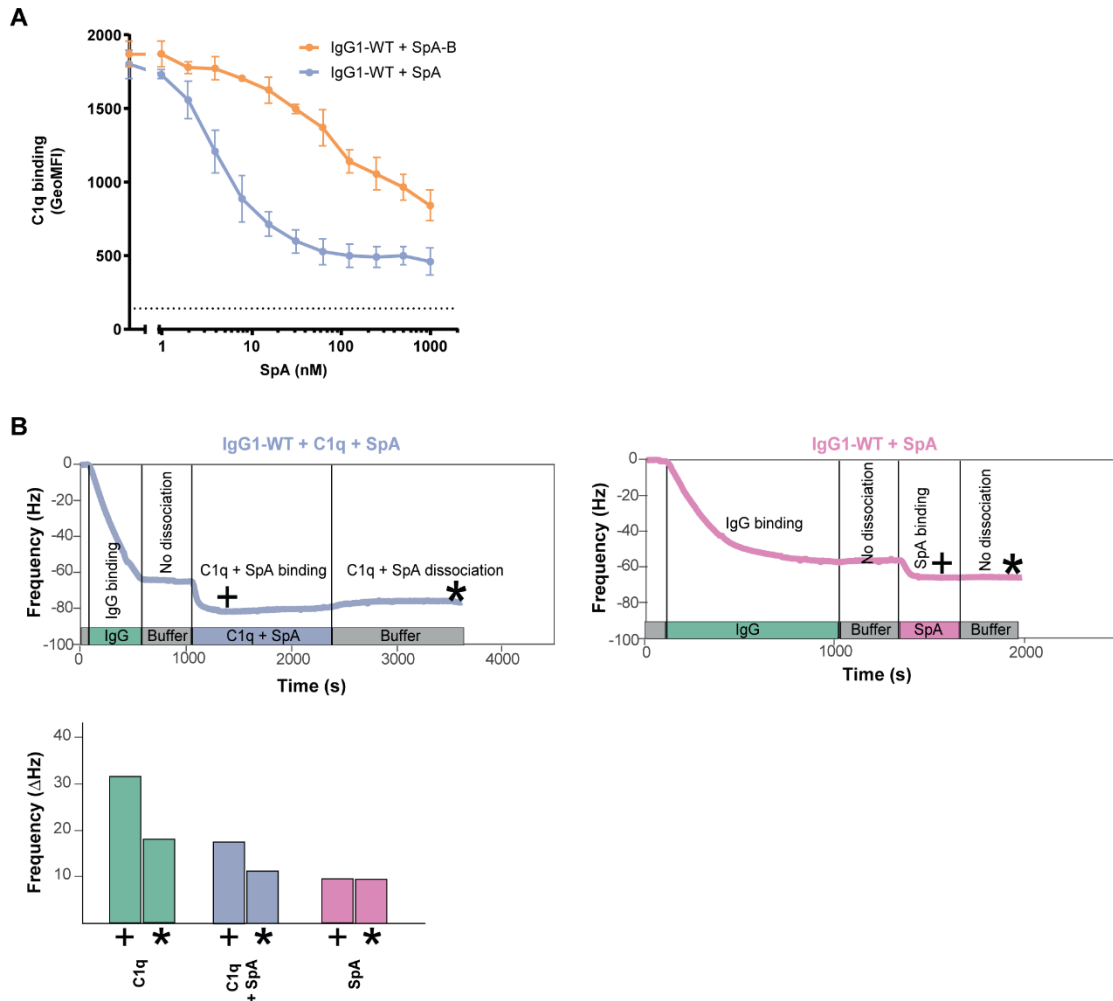


Fig. S5. SpA inhibits binding of C1q to antigen-bound IgGs on target surfaces. (A) C1q binding on anti-DNP IgG1-WT bound to DNP-coated beads after incubation of C1 complex with a concentration range of SpA-B (orange) or SpA (blue), detected with FITC-conjugated rabbit F(ab')₂ anti-human C1q antibody by flow cytometry. The black dotted line shows the background fluorescence from beads that were not incubated with IgG. Data are presented as geometric means \pm SD of at least three independent experiments. (B) QCM sensorgram of C1q binding to anti-DNP IgG1-WT bound to DNP-decorated lipid bilayers in the presence of SpA and SpA binding (in the absence of C1q) to anti-DNP IgG1-WT bound to DNP-decorated lipid bilayers. Bars represent the respective equilibrium level (+) and the level at the end of the dissociation phase (*) (C1q sensorgram is presented in Fig 5A).

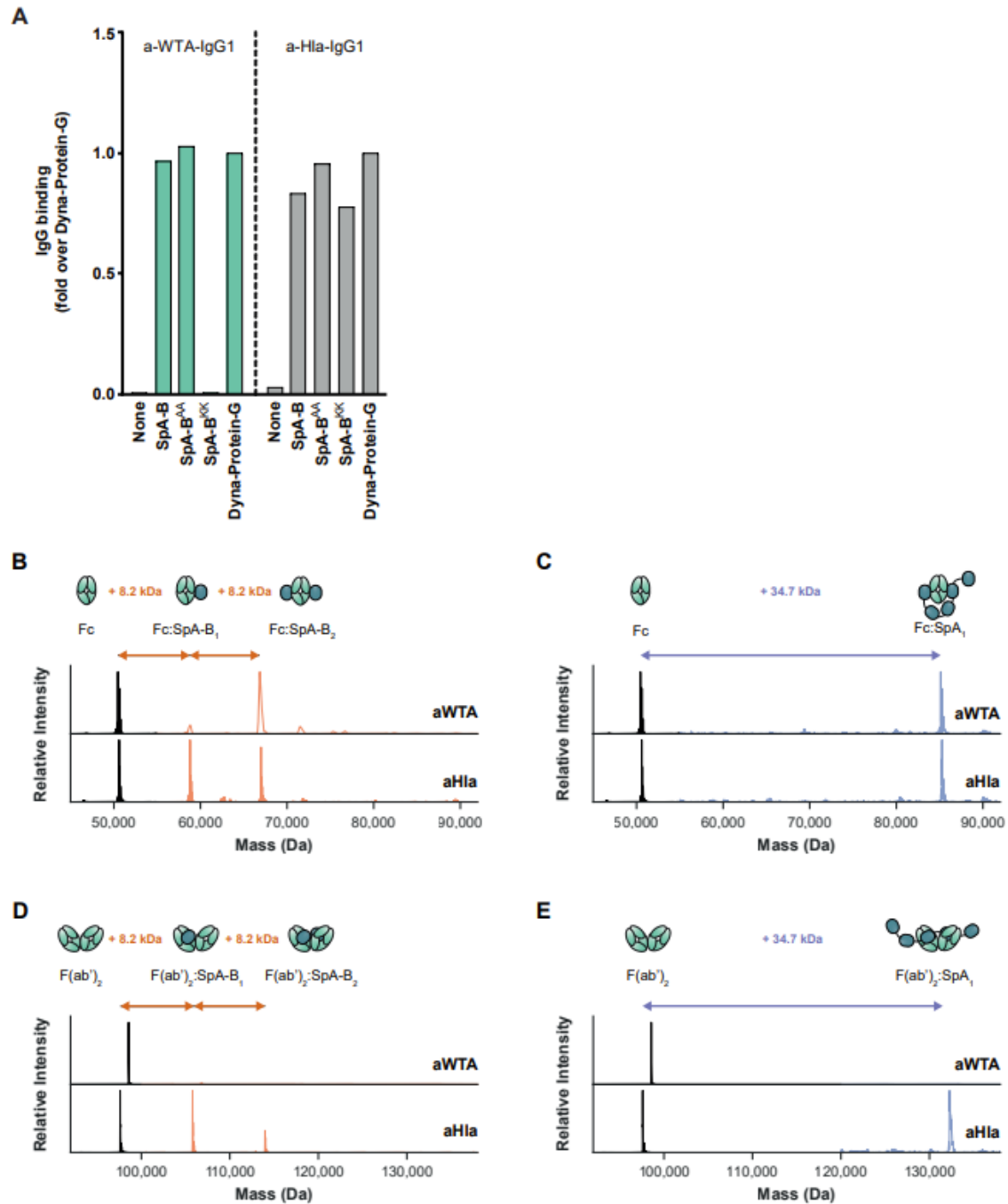


Fig. S6. Human anti-WTA antibodies only bind to SpA via their Fc region. (A) Binding of anti-WTA IgG1 (green) and anti-Hla IgG1 (grey) to beads coated with His-tagged recombinant SpA-B (wild-type), SpA-B^{AA} (that only binds to IgG-Fc region), SpA-B^{KK} (that only binds to IgG-Fab region) or to Protein-G beads. Antibody binding was detected by the use of directly labeled IgG or Alexa Fluor⁶⁴⁷-conjugated goat F(ab')₂ anti-human kappa and was measured by flow cytometry. Protein-G beads served as universal IgG1 and IgG3 binding control. The binding data for anti-Hla IgG1 (VH3 family antibody) was also shown in Fig. S2. (B-E) Deconvoluted native mass spectra of the Fc (B, C) and

F(ab')₂ (D, E) molecules of anti-WTA IgG1 or anti-Hla IgG1 resulting from IdeS digestion measured in absence (black) or in presence of SpA-B (orange) or SpA (blue). To the Fc portion of both antibodies, SpA-B binds 2:1 (B) and SpA binds 1:1 (C). However, only the F(ab')₂ molecule of anti-Hla IgG1 can interact with SpA-B (D) and SpA (E), which bind to these constructs with 2:1 and 1:1 stoichiometry, respectively. The cartoons regarding Fc:SpA₁ and F(ab')₂:SpA₁ binding are speculative, as it is still unknown which SpA domain interacts with which binding site on the IgG molecules.

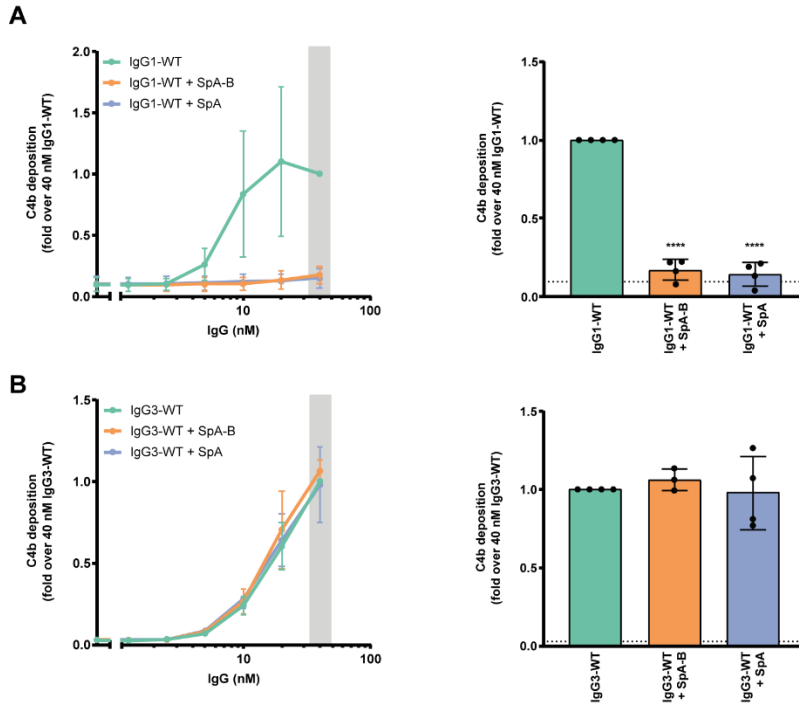


Fig. S7. SpA decreases IgG-mediated C4b deposition on *S. aureus*. (A, B) C4b deposition on Newman $\Delta spa/sbi$ surface after bacteria incubation with IgG1-WT (A) or IgG3-WT (B), 1% Δ IgG/IgM human serum and buffer (green), SpA-B (orange) or SpA (blue), detected with a monoclonal murine anti-human C4d antibody by flow cytometry. Bars represent the same data for the 40 nM IgG concentration only and the black dotted line shows the background fluorescence from bacteria that were not incubated with IgG. Data are presented as fold change over the 40 nM IgG concentration control \pm SD of at least three independent experiments. Statistical analysis was performed using one-way ANOVA to compare buffer condition with SpA-B and SpA conditions and showed when significant as ****P < 0.0001.

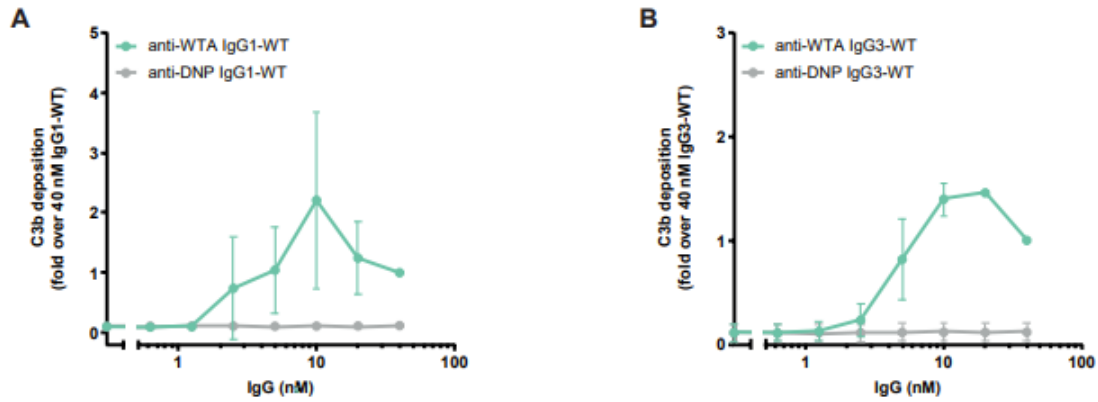


Fig. S8. C3b detection by anti-WTA antibodies reflects the presence of covalently bound C3 products that were deposited upon complement activation. (A, B) C3b deposition on Newman $\Delta spa/sbi$ surface after incubation of bacteria with anti-WTA wild-type (anti-WTA; green line) or anti-DNP wild-type (anti-DNP; grey line) antibodies of IgG1 subclass (A) or of IgG3 subclass (B) in presence of 1% $\Delta IgG/IgM$ human serum, detected with a monoclonal murine anti-human C3d antibody by flow cytometry. Data are presented as fold change over 40 nM concentration of IgG control \pm SD of two independent experiments.

SI Tables

Table S1. Amino acid sequence of SpA-B constructs. The amino acid substitutions that are highlighted in bold abrogate binding of SpA-B^{KK} and SpA-B^{AA} to Fc and Fab domain of human IgG, respectively.

SpA-B construct	Sequence
SpA-B	MADNKFNKEQQNAFYEILHLPNLNEEQRNGFIQSLKDDPSQSANLLAEAK KLNDAQAPK
SpA-B ^{KK}	MADNKFNKE KK NAFYEILHLPNLNEEQRNGFIQSLKDDPSQSANLLAEAKK LNDAQAPK
SpA-B ^{AA}	MADNKFNKEQQNAFYEILHLPNLNEEQRNGFIQSLK AA PSQSANLLAEAK KLNDAQAPK

Table S2. Theoretical and experimental molecular weight values of proteins analyzed by native MS. The mass deviations of ≈ 2.5 kDa for the IgGs are due to the N-glycosylations in the Fc region, whereas the 42 kDa mass difference for C1q is expected due to extensive glycosylation of the α , β and γ subunits.

Species	MW_{theoretical} (Da)	MW_{experimental} (Da)	ΔMW (Da)
SpA-B	8,320	8,188	-132*
SpA-BKK	8,320	8,188	-132*
SpA	34,660	34,663	3
IgG1	146,995	149,217	2,222
IgG1-RGY	147,057	149,831	2,774
IgG2	146,428	149,065	2,636
IgG2-RGY	146,490	149,137	2,647
IgG3	157,219	160,113	2,894
IgG3-RGY	157,281	159,929	2,647
IgG4	146,544	149,181	2,637
IgG4-RGY	146,606	149,237	2,631
C1q	421,437	463,591	42,153

* Corresponding to the deletion of Met1 in the protein sequence.

Table S3. Theoretical and experimental mass values of proteins complexes related to Fig 2A, native mass spectra showing the effect of SpA-B and SpA on IgG1-RGY hexamerization. The theoretical mass of the complex, as calculated using the measured masses of individual subunits, is compared to the experimental mass. For these experiments, instrumental parameters were optimized for the quantification of (IgG)₆ complexes.

Species	M_{theoretical} (kDa)	M_{experimental} (kDa)	Mass error (kDa)
(IgG1) ₁	149.8	149.9	0.07
(IgG1) ₁ :SpA-B ₁	158.0	158.3	0.32
(IgG1) ₁ :SpA-B ₂	166.2	166.6	0.39
(IgG1) ₁ :SpA ₁	184.5	184.8	0.31
(IgG1) ₂	299.7	299.9	0.25
(IgG1) ₃	449.5	449.9	0.39
(IgG1) ₄	599.3	599.8	0.51
(IgG1) ₆	899.0	900.4	1.43

Table S4. Theoretical and experimental mass values of proteins complexes related to Fig 3A, native mass spectra showing the effect of SpA-B and SpA on (IgG1-RGY)₆:C1q assembly. The theoretical mass of the complex, as calculated using the measured masses of individual subunits, is compared to the experimental mass. For these experiments, instrumental parameters were optimized for the quantification of (IgG)₆:C1q complexes.

Species	M_{theoretical} (kDa)	M_{experimental} (kDa)	Mass error (kDa)
(IgG1) ₁	149.8	150.0	0.13
(IgG1) ₁ :SpA-B ₁	158.0	158.2	0.22
(IgG1) ₁ :SpA-B ₂	166.2	166.4	0.22
(IgG1) ₁ :SpA ₁	184.5	184.8	0.35
(IgG1) ₂	299.7	299.9	0.21
(IgG1) ₃	449.5	449.7	0.24
C1q	463.6	463.8	0.17
(IgG1) ₆	899.0	899.9	0.95
(IgG1) ₆ :C1q	1,362.6	1,364.5	1.96

Table S5. Amino acid sequence of the variable and constant heavy and light chains of antibodies produced in this study (5, 6).

	Antibody	Sequence
Variable heavy chain	Anti-DNP IgG	DVRLQESGPGPLVKPSQSLSLTCVSTGYSITNSYYWNWIRQFPGNKLEWMV YIGYDGSNNYNPSLKNRISITRDTSKNQFFLKLNSVTTEDTATYYCARATYY GNYRGFAYWGQGTLVTVSA
	Anti-WTA IgG	EVQLVESGGGLVQPGGSLRLSCSASGFSFNSFWMHWVRQVPGKGLVWIS FTNNEGTTTAYADSVRGRFIISRDNKNTLYLEMNLRGEDTAVYYCARGD GGLDDWGQGTLVTVSS
Variable light chain	Anti-DNP IgG	DIRMTQTTSSLSASLGDRVTISCRASQDISNYLNWYQQKPDGTVKLLIYYTS RLHSGVPSRFSGSGSGTDYSLTISNLEQEDIATYFCQQGNTLPWTFGGGTK LEIK
	Anti-WTA IgG	DIQLTQSPDSLAVSLGERATINCKSSQSIFRTSRNKNLLNWYQQRPGQPPR LLIHWASTRKSQVDFRFSGSGFGTDFTLTITSLQAEDVAIYYCQQYFSPPYT FGQGTKLEIK
Constant heavy chain	IgG1	ASTKGPSVFPLAPSSKSTSGGTAALGCLVKDYFPEPVTVSWNSGALTSKV HTFPAVLQSSGLYSLSSVTVPSSSLGTQTYICNVNHKPSNTKVDKKEPK SCDKTHTCPPCPAPELLGGPSVFLFPPKPKDTLMISRTPEVTCVVDVSHEDPEVQ DPEVKFNWYVDGVEVHNAKTKPREEQYNSTYRVVSVLTVLHQDWLNGKE YKCKVSNKALPAPIEKTISKAKGQPREPQVYTLPPSREEMTKNQVSLTCLVK GFYPSDIAVEWESNGQPENNYKTTTPVLDSDGSFFLYSKLTVDKSRWQQG NVFSCSVMHEALHNHYTQKSLSLSPGK
	IgG2	ASTKGPSVFPLAPCSRSTSESTAALGCLVKDYFPEPVTVSWNSGALTSKVH TFPAVLQSSGLYSLSSVTVPSSNFGTQTYTCNVDHKPSNTKVDKTVKRC CVECPCPAPPVAGPSVFLFPPKPKDTLMISRTPEVTCVVDVSHEDPEVQ FNWYVDGVEVHNAKTKPREEQFNSTFRVSVLTVVHQDWLNGKEYKCKV SNKGLPAPIEKTISKTKGQPREPQVYTLPPSREEMTKNQVSLTCLVKGFYPS DIAVEWESNGQPENNYKTTTPMLDSDGSFFLYSKLTVDKSRWQQGNVFC SVMHEALHNHYTQKSLSLSPGK
	IgG3	ASTKGPSVFPLAPCSRSTSESTAALGCLVKDYFPEPVTVSWNSGALTSKV HTFPAVLQSSGLYSLSSVTVPSSSLGTQTYTCNVNHKPSNTKVDKRVKELK TPLGDTTHTCPRCPEPKSCDTPPPCPRCPEPKSCDTPPPCPRCPEPKSCD TPPPCPRCPAPELLGGPSVFLFPPKPKDTLMISRTPEVTCVVDVSHEDPEV QFKWYVDGVEVHNAKTKPREEQYNSTFRVSVLTVLHQDWLNGKEYKCK VSNKALPAPIEKTISKTKGQPREPQVYTLPPSREEMTKNQVSLTCLVKGFYPS SDIAVEWESSGQPENNYNTTPMLDSDGSFFLYSKLTVDKSRWQQGNIFS CSVMHEALHNRFQKSLSLSPGK
	IgG4	ASTKGPSVFPLAPCSRSTSESTAALGCLVKDYFPEPVTVSWNSGALTSKVH TFPAVLQSSGLYSLSSVTVPSSSLGTQTYTCNVDHKPSNTKVDKRVESKY GPPCPSCPAPPEFLGGPSVFLFPPKPKDTLMISRTPEVTCVVDVSDQEDPEV QFNWYVDGVEVHNAKTKPREEQFNSTYRVVSVLTVLHQDWLNGKEYKCK VSNKGLPSSIIEKTISKAKGQPREPQVYTLPPSQEEMTKNQVSLTCLVKGFY PSDIAVEWESNGQPENNYKTTTPVLDSDGSFFLYSRLTVDKSRWQEGNVF SCSVMHEALHNHYTQKSLSLSPGK
Constant light chain (<i>kappa</i>)	IgG1, 2, 3, 4	RTVAAPSVFIFPPSDEQLKSGTASVVCLLNFFYPREAKVQWKVDNALQSGN SQESVTEQDSKSTYLSSTLTLSKADYEKHKVYACEVTHQGLSSPVTKSF NRGEC

SI References

1. C. A. Diebold, *et al.*, Complement is activated by IgG hexamers assembled at the cell surface. *Science* **343**, 1260–1263 (2014).
2. K. D. White, M. B. Frank, S. Foundling, F. J. Waxman, Effect of immunoglobulin variable region structure on C3b and C4b deposition. *Mol. Immunol.* **33**, 759–768 (1996).
3. D. Ugurlar, *et al.*, Structures of C1-IgG1 provide insights into how danger pattern recognition activates complement. *Science* **359**, 794–797 (2018).
4. X. T. Fang, D. Sehlin, L. Lannfelt, S. Syvänen, G. Hultqvist, Efficient and inexpensive transient expression of multispecific multivalent antibodies in Expi293 cells. *Biol. Proced. Online* **19**, 1–9 (2017).
5. M. L. Gonzalez, M. B. Frank, P. A. Ramsland, J. S. Hanas, F. J. Waxman, Structural analysis of IgG2A monoclonal antibodies in relation to complement deposition and renal immune complex deposition. *Mol. Immunol.* **40**, 307–317 (2003).
6. S. M. Lehar, *et al.*, Novel antibody-antibiotic conjugate eliminates intracellular *S. aureus*. *Nature* **527**, 323–328 (2015).
7. J. Strasser, *et al.*, Unraveling the Macromolecular Pathways of IgG Oligomerization and Complement Activation on Antigenic Surfaces. *Nano Lett.* **19**, 4787–4796 (2019).
8. S. A. Zwarthoff, S. Magnoni, P. C. Aerts, K. P. M. van Kessel, S. H. M. Rooijackers, Depletion of IgG and IgM from human serum as naive complement. *Methods Mol. Biol.*, in press.